J Fluoresc (2007) 17:249–255
DOI 10.1007/s10895-007-0166-4

ORIGINAL PAPER

Potassium Ion Induced Changes of Crystal Structure and Fluorescence of a Crown Ether

Qiu- Xian Ren · Vincent Douglass III · Wenying Xu · Michal Sabat · A. Periasamy · J. N. Demas · B. A. DeGraff

Received: 26 May 2005 / Accepted: 1 February 2007 / Published online: 29 March 2007

Abstract Luminescence properties and the x-ray structures of the fluorescent crown ether, 16-anthracen-ylmethyl-1,4,7,10,13-pentaoxa-16-aza-cyclooctadecane (CEA) and its complex with potassium hexafluorophosphate (CEAK) have been obtained. In the solid state CEAK gives a structured blue emission and CEA gives a broad structureless green emission. The differences in luminescence behavior are explained on the basis of crystal packing. X-ray analysis shows that every two adjacent anthracene moieties in CEA form a sandwich-like anti-parallel dimer; the green-structureless emission then arises from the π-π stack of the aromatic rings. In CEAK, disruption of the π-π stacking structure forces a large separation between the anthracene rings, which yields an anthracene monomer emission. Luminescence lifetime data support the assignments.

Keywords Potassium · Ion sensor · Exciplex · Anthracene · Crown ether

Introduction

Recently, there has been a considerable interest in fluorescent cation sensors due to their extensive applications in many chemical and biological processes [1–3]. Generally, sensors of this kind consist of a fluorophore linked to an ionophore. The ionophore is the recognition moiety, which is responsible for the selectivity and efficiency of binding to the cation. The fluorophore acting as a signaling moiety can transduce the recognition event into an optical signal.

Crown ethers have attracted considerable attention because these ionophores can bind metal ions selectively based on the size and fit within the macrocyclic cavity [1–4]. Anthracene has frequently been used as a signaling moiety since its luminescence can be easily modulated. These promising spectroscopic properties have stimulated extensive research on the anthracene-based crown ether cation sensors [5–8].

Most of these sensors were concerned with cation-induced changes of fluorescence properties of anthracene in solution. However, there have been a few reports on the effect of cation complexation on solid-state luminescent properties. Desvergne and Bouas-Laurent described the bis(anthraceno)-crown ether complex with metal cations in the crystalline state [9, 10]. In contrast to our system, their research showed that the cations altered the conformation and brought the aromatic moieties close enough together to overlap with a resultant anthracene excimer-like fluorescence.

In reality there is considerable argument over the detailed emissions of solid state aromatic crystals [11–13]. One could have a pure excimer with no ground state counterpart, a dimer emission, or an interacting ground state that is not so strong as to represent a dimer but does perturb the monomer states. Further, the extent of the interactions and the luminescence are critically dependent on remarkably small changes in the packing [14]. Additionally, the configurations vary depending on whether the interacting anthracene moieties were generated by crystallization, by photodissociation of the photodimers in the solid state, or by microcrystallization in solution. Regardless, the common usage in the luminescence sensor area is that the low energy, broad structureless

Q.-X. Ren · V. Douglass III · W. Xu · M. Sabat · J. N. Demas (✉)
Department of Chemistry, University of Virginia,
Charlottesville, VA 22904-4319, USA
e-mail: demas@virginia.edu

A. Periasamy
W.M. Keck Center for Cellular Imaging, University of Virginia,
Charlottesville, VA 22904-4319, USA

B. A. DeGraff
Department of Chemistry, James Madison University,
Harrisonburg, VA 22807, USA

emissions are the result of excimer formation even though this is clearly incorrect in some cases. It is not our goal here to get into the details of this controversy for our system. We will generally refer to broad structureless emissions as excimer-like.

As part of our interest in luminescence-base sensors, we examined 16-anthracen-ylmethyl-1,4,7,10,13-pentaoxa-16-aza-cyclooctadecane (CEA), which was originally designed as a very sensitive cation fluorescent sensor based on photo induced electron transfer (PET) [15]. The emission spectrum of CEA in solution with and without potassium ion corresponds to the typical blue luminescence of the anthracene chromophore, although the luminescence intensity varied with the degree of complexation. In the uncomplexed form the lone electron pair on the aza crown partially quenched the anthracene by PET; when the lone pair was tied up in metal ion binding PET was suppressed. However, we found huge differences in the solid-state emission spectra of CEA and its complex with potassium hexafluorophosphate (CEAK). CEA gave a striking green emission in contrast to CEAK, which gave the normal blue anthracene emission. We show that the different packings of the molecules in the crystals are responsible for these differences.

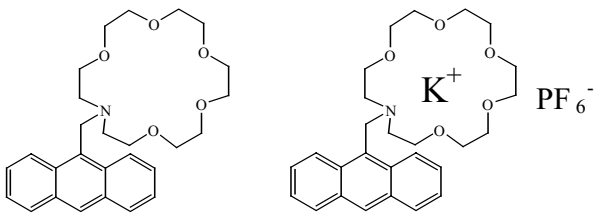

CEA **CEAK**

Experimental section

Materials

9-(Chloromethyl)-anthracene, 1-aza-18-crown-6 and potassium hexafluorophate (Aldrich Chemical Co.) were used as received.

Synthesis

N-(9-anthryl)-aza-18-crown-6 (CEA) was prepared as described earlier [16]. 9-(Chloromethyl)-anthracene and 1-aza-18-crown-6 with potassium carbonate were refluxed in toluene for 24 hr. Crystallization from ethanol afforded CEA as yellow needles. The melting point of 92.5–93°C mp agreed well with the reported 93°C [16]. NMR agreed with the literature [16]. Refluxing of CEA and KPF_6 in methanol for 3 hr, followed by collection of the precipitate, provided the potassium complex of N-(9-anthryl)-aza-18-crown-6 (CEAK). Crystals of CEAK for X-ray determination were prepared by recrystallization from dry methanol.

Table 1 Crystallographic data

	CEA	CEAK
emp formula	$C_{27}H_{35}NO_5$	$C_{27}H_{35}F_6KNO_5P$
color	Pale Yellow	Colorless
formula weight	453.56	637.63
T(K)	153(2)	293(2)
λ(Å)	0.71073	0.71073
cryst system	Monoclinic	Monoclinic
space group	$P2_1/c$ (No.14)	$P2_1/c$ (No.14)
a(Å)	10.0117(4)	11.1094(6)
b(Å)	9.8538(4)	11.3338(6)
c(Å)	23.742(1)	23.786(1)
β(deg)	92.646(1)°	96.573(1)
V(Å^3)	2339.7(2)	2975.2(3)
Z	4	4
d_{calcd}, Mg/m^3	1.288	1.424
Θ range, deg	1.72–32.53	1.72–32.54
no. of reflns collected	31755	40226
no. of reflns with $I > 2\sigma(I)$	8472	10756
$R1$, w$R2$	0.0582, 0.1353	0.0575, 0.1232
GOF	0.961	0.876

Crystal structure determination

All X-ray diffraction experiments were carried out on a Bruker SMART APEX CCD diffractometer using MoKα radiation ($\lambda = 0.71073$ Å). Pertinent crystallographic data for CEA and CEAK are listed in Table 1. The structure solution and full-matrix least-squares refinement based on F^2 were performed using the SHELXL program package [17]. All non-hydrogen atoms were refined with anisotropic thermal displacement parameters, whereas the hydrogen atoms were subject to an isotropic refinement.

Luminescence measurements

Emission and excitation spectra were recorded on a Spex Fluorolog 1680 fluorometer. Low temperature measurements were made with an optical Dewar flask. The lifetime of CEA was measured using a pulsed VSL-377 nitrogen laser and a Tektronix TDS-540 digital oscilloscope. Data were collected after averaging 300 decay curves. The decays were double exponential and were fit by nonlinear least squares to

$$D(t) = K_1 \exp(-t/\tau_1) + K_2 \exp(-t/\tau_2) \quad (1)$$

The relative contributions of each component to the total emission were calculated from

$$f_1 = K_1\tau_1/(K_1\tau_1 + K_2\tau_2) \quad (2a)$$

$$f_2 = K_2\tau_2/(K_1\tau_1 + K_2\tau_2) \quad (2b)$$

The preexponential weighted lifetime [18] was computed from

$$\tau_{pw} = f_1\tau_1 + f_2\tau_2 \quad (3)$$

For the CEAK, Fluorescence Lifetime Imaging Microscopy (FLIM) was used to measure the spectrally resolved lifetime of a single crystal. Two-photon excitation of the sample using 790 nm was carried out by a Titanium Sapphire Laser (Coherent, Inc.). The FLIM apparatus included a Nikon TE 3000 epi-fluorescence microscope for Biorad Radiance 2100 Confocal/Multiphoton Microscopy, band pass filter (450/80 nm or 515/30 nm), and a time correlated single photon counting system based on a Becker & Hickl GmbH, (http://www.beckerhickl.de) company photon-counting module (TCSPSC, SPC-730) using the Becker & Hickl supplied software[14, 19]. The decay curves of each pixel were gathered and analyzed by single or double exponential equations. At the count levels for each pixel, a single exponential satisfactorily fit the decay curves, and only single component decays are reported. The lifetime of each pixel was coded by false color.

Luminescence measurements of CEA were made in several solvents of varying polarities at both room and liquid nitrogen temperatures. Solvents included absolute ethanol-methanol (4:1; V:V) (EtOH-MeOH), *n*-hexane, and diethyl ether. All solvents were of reagent grade and were used without further purification.

Results and discussion

Crystal structure

The X-ray structures of CEA and CEAK are shown in Fig. 1. Whereas the anthracyl moiety of CEA points away from the center of the macrocycle, it is tucked under the aza crown unit in CEAK. The K···C8 distance of 3.226 Å in the complex indicates an interaction between the K^+ ion and the aromatic system. The average K···O distance for the crown ether contacts is 2.81 Å and the K···N separation is 3.04 Å, slightly shorter than that of the 3.20 Å found in a bibracchial diaza crown with two anthracyl groups [20]. An interesting feature of CEAK is the presence of a relatively short C–H···O contact involving the α-hydrogen atom of the anthracene moiety (H8) and the oxygen atom O5 of the macrocycle. The geometry of this hydrogen bond is very similar to that observed in the bis(anthracyl) complex [15]. Thus, the C···O separation and the C–H···O angle in CEAK are 3.533 Å and 151.1°, respectively, whereas in the bis(anthracyl) analog the distances are 3.54 and 3.58 Å with angles of 152.7 and 156.7°. The opposite face of the macrocycle is flanked by a PF_6^- counter-ion, disordered between two orientations related by a rotation of about 45°. The shortest K···F contact is 2.797 Å.

Figure 2 shows the unit cell content for each structure projected along the a axis. Interestingly, although CEA and CEAK crystallize in unit cells with similar metric parameters and identical space groups, the arrangement of the molecules in these unit cells is very different. The most noticeable difference concerns the adjacent anthracene rings, which form sandwich-like dimers in CEA. The two adjacent

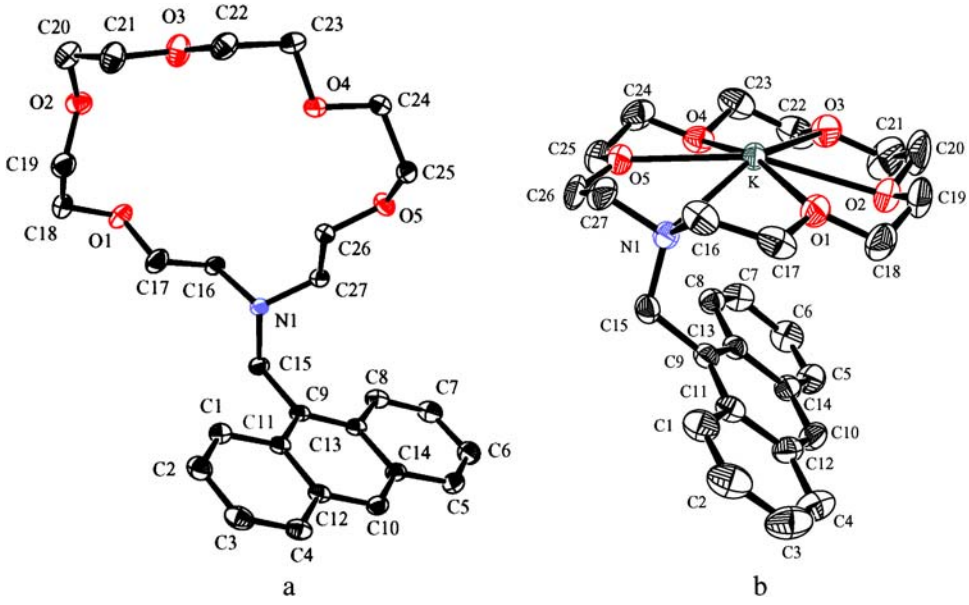

Fig. 1 ORTEP plot of CEA (a) and CEAK (b). Thermal ellipsoids are shown at the 50% (CEA) and 30% (CEAK) probability levels

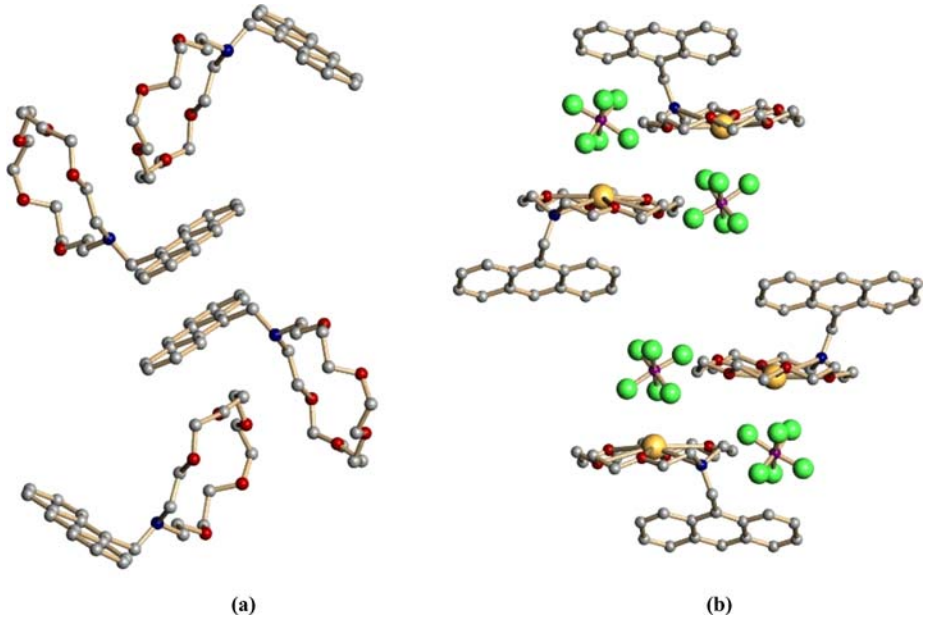

Fig. 2 The unit content of CEA (a) and CEAK (b) projected along a axis

anthracenes (Fig. 3), related by an inversion center, have interplanar C · · · C separations ranging between 3.52–3.66 Å. The displacement from the ideal overlap is about 1.2 Å along the long and short axes of the anthracene ring system. In contrast, the anthracene moieties are quite widely separated in CEAK, where the potassium and hexafluorophosphate ions in the crystal lattice exhibit strong electrostatic interactions. These strong electrostatic forces, as well as the presence of the bulky counter-ion, affect the π-π stacking and result in the absence of any significant overlap between the CEAK anthracyl groups.

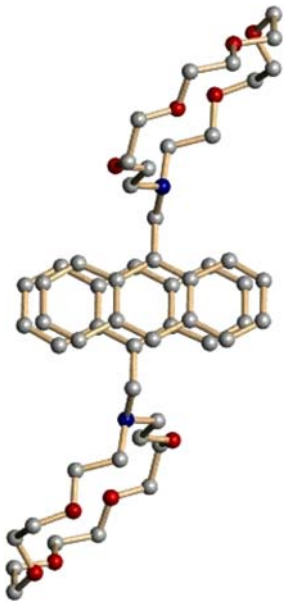

Fig. 3 Projection of the CEA molecule normal to the plane of the anthracene moiety

Fluorescence emission spectra

Figure 4 shows the room temperature emission spectra of solution CEAK and crystalline CEAK and CEA. Crystalline CEA emits green and the emission spectrum is structureless with a peak at 525 nm. Crystalline CEAK gives a blue-structured emission with a maximum at about 420 nm, which is very similar to that of methanol solutions of CEA or CEAK except for a slight red shift. The attenuation of the high energy band in the crystal around 400 nm arises from strong self-absorption in the crystal due to the high optical density in the uv. PET quenching could be occurring in solid CEA and could be reduced in CEAK. However, our measurements do not allow an assessment of this. We can only say that PET, if present, is not very efficient at deactivating the emission of solid CEA.

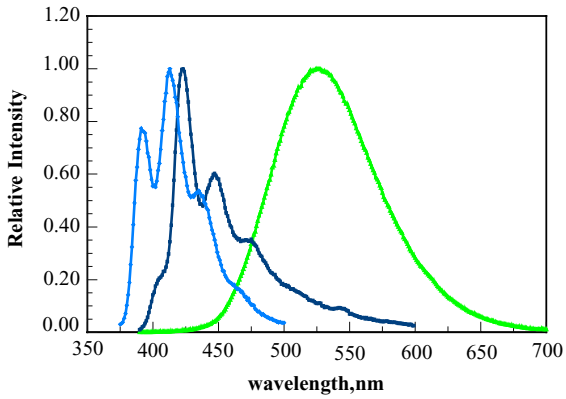

Fig. 4 Normalized room temperature emission spectra of solution CEAK and crystalline CEAK and CEA. The emissions are blue (solution CEAK), dark blue (crystalline CEAK), and green (crystalline CEA)

It has been found that the position and appearance of the fluorescence spectra of crystalline aromatic hydrocarbons has a direct relationship to the molecular orientation in the crystal lattice [21, 22]. There are two types of aromatic crystal lattices: Type A, where the π-orbital overlap of adjacent parallel molecules is restricted by both large molecular separation (interplanar separation of more than 4 Å) and large angles of inclination of the molecular planes with respect to each other. The fluorescence spectra of these kinds of crystals are structured and only slightly shifted relative to the solution spectra. In type B, the molecules are arranged either in a pair configuration or along a stack [21] with an interplanar distance of about 3.5 Å. The B crystal emission spectra are structureless and red shifted dramatically with respect to the spectrum observed in dilute solutions. These emissions are similar to excimer emissions seen in concentrated solutions

$$D^* + D \rightarrow D_2^*(\text{Excimer}) \rightarrow 2D + h\nu$$

and have been assigned to intracrystal excimer formation.

CEA has a typical emission of type B anthracene derivatives, which is consistent with the crystal structure. Figure 3 shows the close pair stacking of anthracene similar to those seen in type B crystals. The close proximity and orientation of the two ring systems, which is consistent with a type B structure, facilitates the intermolecular π orbital interaction and sets them up for easy excited state dimer formation.

In marked contrast, the ionic species in CEAK disrupt the π stacking and prevent close proximity of the two rings. Thus, addition of K transforms the excimer-like emission into the structured anthracene monomer emission typical of type A crystals.

A question is whether the ground state of the anthracenes in CEA can be thought of as a dimer or as just two weakly interacting monomers. In principle, absorption spectra would reveal the presence of a ground state dimer. Due to the difficulty of obtaining solid-state absorption spectra, crystal excitation spectra can reveal much of the same information. As shown in Fig. 5, uncorrected excitation spectra of CEA extended to longer wavelengths than CEAK. Assuming that CEAK, with its isolated anthracene, has the absorption of an anthracene monomer, the red shift of the absorption edge in CEA reveals the presence of new low energy absorptions, which implies the extension of conjugation of anthracene monomers (i.e. a weakly bounded ground-state dimer).

The common view is that quenching of CEA is via PET from the unpaired nitrogen electrons. In the current system, we considered the possibility of a low lying n-π^* excited state (nitrogen non-bonding electron to the anthracene π^* orbital) as being responsible for the quenching. [1, 23] Potassium ion binding would push the n-π^* state above the anthracene π-π^* state and allow a normal anthracene π-π^* emission. If this were the case, we might expect the appearance of an

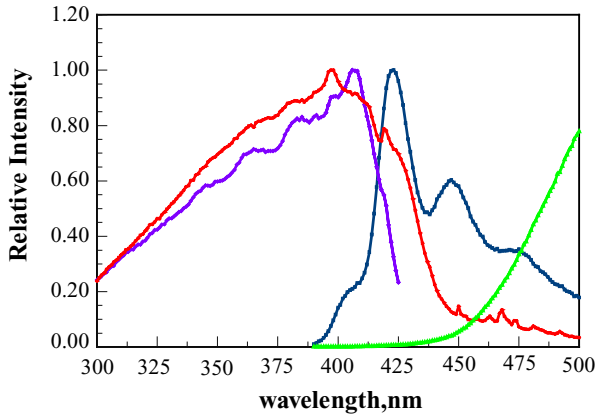

Fig. 5 Emission and excitation spectra of crystalline CEAK and CEA. Red and blue are excitation spectra of CEA and CEAK respectively. Dark blue and green are the emission spectra of CEAK and CEA respectively

n-π^* luminescence in CEA at low temperatures. This would be particularly likely with increasingly weakly interacting solvents such as *n*-hexane that would lower the energy of the n-π^* state. However, the emission spectra of CEA in EtOH-MeOH, diethyl ether and n-hexane at 77 K revealed only the normal beautifully structured blue anthracene emission even for diethyl ether at 10^{-3} M. In no case were any new bands seen, and the anthracene emission was always intense. Therefore, we conclude that quenching of the emission of CEA is not by the presence of a low-lying n-π^* state. We cannot say anything about the degree of PET in low temperature glasses other than it does not strongly quench the CEA emission.

The absence of PET quenching of CEA in low-temperature glasses is consistent with the familiar shutting down of full charge separated states on going to many low temperature glasses. In low-temperature glasses, solvent dipole rotations are eliminated, which precludes their stabilizing formation of the incipient ion pair and results in a greatly decreased electron transfer rate over fluid solutions [24]. A similar effect is also probably operative in crystalline CEA where there is no solvent to reorganize and little opportunity for significant motion of the excited molecule in the crystal lattice.

The room temperature emissions in these solvents were all anthracene-like at concentrations up to about 10^{-5} M. Diethyl ether at 10^{-3} M did, however, exhibit an excimer-like emission at 525 nm with an intensity comparable to the monomer emission. Given the short lifetime of anthracene, these results indicate that ground state dimerization is occurring in this solvent. In order to see a true excimer by bimolecular interaction of an excited and a ground state molecule, the rate constant for excimer formation would have to be on the order of $> 5 \times 10^{11}$ M^{-1} s^{-1}, which is improbably

Table 2 Lifetimes of CEA at different monitoring wavelengths

Monitoring Wavelength, nm	500	525	550
Double Exponential Decay fit	T1 = 16ns f1 = 0.40	T1 = 20ns f1 = 0.37	T1 = 18ns f1 = 0.35
	T2 = 100ns f2 = 0.60	T2 = 98ns f2 = 0.63	T2 = 96ns f2 = 0.65
Average Lifetime, ns	66	69	69

high. This result is consistent with the formation of a weak ground state dimer in the CEA crystals.

Excited state lifetimes of crystalline CEA

Table 2 shows the decay data for crystalline CEA along with the preexponential weighted excited state lifetime recorded at different wavelengths. The lifetimes are essentially wavelength independent. The longer lifetimes, especially the longest one, are consistent with excimer-like emissions. We cannot exclude some type of trap site as the source of the emission, but the spectral distribution and lifetimes are consistent with an excited state dimer. The packing of molecules in crystalline CEA shows that every two adjacent anthracene moieties form a sandwich anti-parallel dimer with both anthracenes being equivalent. Thus, one might have expected a single lifetime. Dual excimer lifetimes are common in crystals and even in solution at high concentrations. In solution, different dimer conformations can result with a concomitant difference in excited state dimer lifetimes [12]. In crystalline 9-cyano-anthracene, two excimer lifetimes were found (40 and 167 ns at 77 K) [25] even though the defect-free crystal should have only one conformation. The origin of the second decay time in our case is unknown but may arise from a dimer in a defect site. In CEA, the two lifetimes may also arise from defects.

Excited-state lifetimes of crystalline CEAK

The lifetimes of CEAK are several nanoseconds, which is consistent with anthracene monomers. These lifetimes are much less than that of CEA and are not measurable on our pulsed nitrogen laser lifetime instrument; therefore, these lifetimes were measured by FLIM.

With FLIM we obtain a decay curve and lifetime for every pixel on the crystal image. To present this data, the decay times on the image are presented in false colors and the lifetime distribution is displayed in Fig. 6. The lifetime distribution of CEAK monitored at 450 nm was quite narrow (Fig. 6A) with a peak at about 2 ns. Monte Carlo simulations show that this distribution is about what is expected statistically for time correlated single photon counting decay curves with the number of photons observed in our decays. Thus, we conclude that the decay is essentially single exponential when observed at 450 nm. Lifetime images focused on the interior of the crystal displayed a distribution of lifetimes indistinguishable from the surface.

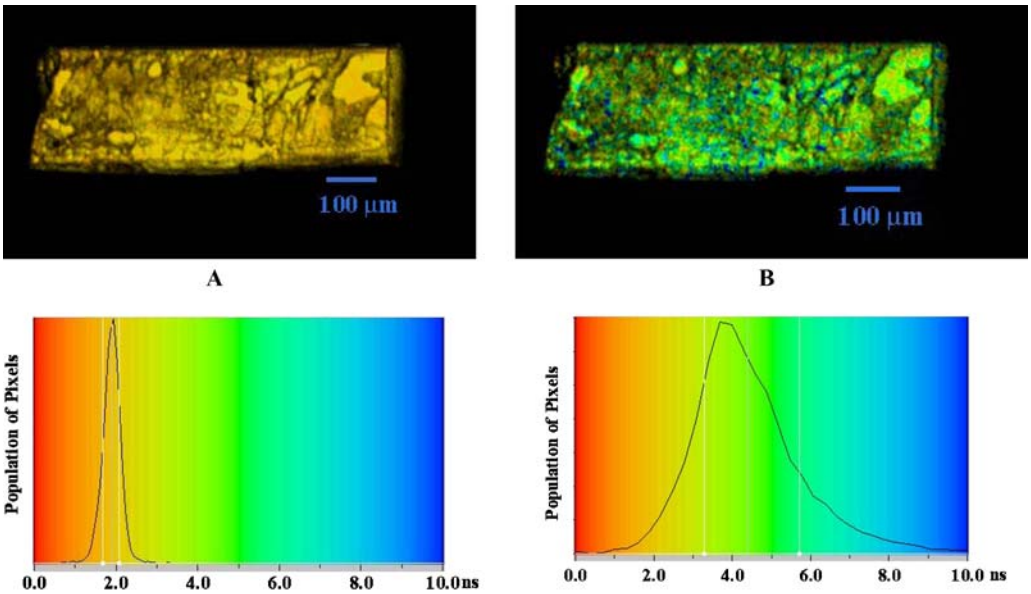

Fig. 6 Top: Two-photon lifetime images of CEAK monitored at (A) 450/80 nm, and (B) 515/30 nm band pass filter. Bottom: Lifetime distribution of the image A (left) and B (right). Note: Lifetime of each pixel was coded by different colors for visual effect

Therefore, surface defects do not appear to affect the lifetime.

In contrast, the lifetime distribution monitored at 515 nm was very broad with a peak at about 4 ns; this difference and heterogeneity is clearly visible in the color distribution of Fig. 6B. Due to the overlap of absorption and emission spectra [26], other monomers in the crystal can reabsorb the primary emission and reemit. The net effect is depletion of the blue and enhancement of the redder emission with increased lifetimes for the longer wavelength emissions due to multiple reabsorption-reemissions. While images at 450 nm give mainly the primary emission, the lifetime image collected at 515 nm contains reemissions with longer apparent lifetimes.

Conclusions

CEA demonstrates dramatically different solid state luminescence properties depending on whether the crown is associated with a K ion or not. In the absence of potassium, the anthracene can π stack in the crystal and give rise to an intense long-lived green excimer-like emission. With the crown coordinated to K, π stacking is blocked and the isolated anthracenes give a short lived blue emission characteristic of the monomeric anthracene. In dilute solutions, both CEA and the potassium salt give identical monomer emissions.

Acknowledgments We thank the NSF (CHE 00–994777 and 04–10061) for support of this work.

Reference

1. de Silva A Prasanna, Gunaratne HQN, Gunnlaugsson T, Huxley AJM, McCoy CP, Rademacherand JT, Rice TE (1997) Signaling Recognition Events with Fluorescent Sensors and Switches. Chem Rev 97(5):155–1566
2. de Silva A Prasanna, Fox DB, Huxley AJM, Moody TS (2000) Combining luminescence, coordination and electron transfer for signaling purposes. Coord Chem Rev 205:41–57
3. Valeur B, Leray I (2000) Design principles of fluorescent molecular sensors for cation recognition. Coord Chem Rev 205:3–40
4. Steed JW (2001) First- and second-sphere coordination chemistry of alkali metal crown ether complexes. Coord Chem Rev 215:171–221
5. Tucker J, Bouas-Laurent H, Marsau P, Riley SW, Desvergne J-P (1997) A novel crown ether-cryptand photoswitch. Chem Commun 13:1165–1166
6. Marquis D, Desvergne J-P, Bouas-Laurent H (1995) Photoresponsive Supramolecular Systems: Synthesis and Photophysical and Photochemical Study of Bis-(9,10-anthracenediyl)coronands AAOnOn. J Org Chem 60(24):7984–7996
7. Bouas-Laurent H, Castellan A, Daney M, Desvergne J-P, Guinand G, Marsau P, Riffaud MH (1986) Cation-directed photochemistry of an anthraceno-crown ether. J Am Chem Soc 108(2):315–317
8. Kubo K, Ishige R, Sakurai T (1998) Synthesis and complexation behavior of N,N'-bis(9-anthrylmethyl)-1,4,10,13-tetraoxa-7,16-diazacyclooctadecane. Heterocycles 48(2):347–351
9. Fages F, Desvergne J-P, Bouas-Laurent H, Lehn J-M, Barrans Y, Marsau P, Meyer M, Albrecht-Gary A-M (1994) Synthesis, structural, spectroscopic, and alkali-metal cations complexation studies of a bis-anthracenediyl macrotricyclic ditopic receptor. J Org Chem 59(18):5264–5271
10. Marsau P, Bouas-Laurent H, Desvergne J-P, Fages F, Lamotte M, Hinschberger J (1988) Solid state interactions in anthracenocryptands and crown-ethers, x-ray structure analysis and fluorescence emission of the free ligands and two of their complexes. Mol Cryst Liq Cryst Inc Nonlin Opt 156(Pt. A):383–392
11. Chandross EA, Ferguson J, McRae EG (1966) Absorption and emission spectra of anthracene dimers. J Chem Phys 45(10):3546–3553
12. Chandross EA, Ferguson J (1966) Absorption and excimer fluorescence spectra of sandwich dimers of substituted anthracenes. J Chem Phys 45(10):3554–3563
13. Ferguson J (1966) Absorption and emission spectra of the perylene dimer. J Chem Phys 44(7):2677–2683
14. Becker HD, Sandros K, Skelton BW, White AH (1981) Relationship between fluorescence and molecular geometry. The stereochemistry of 9,10-dihydroanthracenes and the effect of excimer geometry on the emission spectra of crystalline anthracenes. J Phys Chem 85(20):2930–2933
15. de Silva A Prasanna, de Silva SA (1986) Fluorescent signaling crown ethers: switching on of fluorescence by alkali metal ion recognition and binding in situ. J Chem Soc Chem Commun 23:1709–1710
16. Bissell RA, Calle E, de Silva A Prasanna, de Silva SA, Gunaratne HQN, Habib-Jiwan JL, Peiris SLA, Rupasinghe RADD, Samarasinghe TKSD et al. (1992) Luminescence and charge transfer. Part 2. (Aminomethyl)anthracene derivatives as fluorescent PET (photoinduced electron transfer) sensors for protons. J Chem Soc Perkin Trans 2: Phys Org Chem (1972–1999) 9:1559–64
17. Sheldrick GM (1997) SHELXTL Version 5.1 Reference Manual. Bruker AXS: Madison, WI
18. Carraway ER, Demas JN, DeGraff BA (1991) Luminescence Quenching Mechanism for Microheterogeneous Systems. Anal Chem 63:332–336
19. Chen Y, Periasamy A (2004) Characterization of two-photon excitation fluorescence lifetime imaging microscopy for protein localization. Micros Res Tech 63(1):72–80
20. De Wall SL, Meadows ES, Barbour LJ, Gokel GW (1999) Intramolecular C-H hydrogen bonding reduces cation complexation strength in a fluorescent crown ether. Chem Commun 16:1553–1554
21. Stevens B (1962) Effects of molecular orientation on fluorescence emission and energy transfer in crystalline aromatic hydrocarbons. Spectrochimica Acta 18:439–48
22. Robertson JM (1951) The measurement of bond lengths in conjugated molecules of carbon centers. Proc Roy Soc (London) A207:101–110
23. Shim M, Ishimaru S, Tsunooka M (1991) Cation-Sensitive Fluorescence of Polymers Bearing Crowned Acetophenone Moieties. Macromolecules 24:1690–1691
24. Wasielewski Michael R, Johnson Douglas G, Svec Walter A, Kersey Kristin M, Minsek David W (1988) Achieving high quantum yield charge separation in porphyrin-containing donor-acceptor molecules at 10 K. J Am Chem Soc 110(21):7219–21
25. Jones AC, Janecka-Styrcz K, Williams JO (1982) Fluorescence lifetimes and time-resolved spectroscopy of 9-cyanoanthracene crystals in the temperature range 77–300 K. J Photochem 19(2):163–172
26. Ahmad-Bitar RN, Bulos BR, Hassan IR, Jomah MH (1986) Temperature and wavelength dependence of the fluorescence lifetime of anthracene crystals. Japn Appl Phys Part 1 25(4):583–585